NMR Microimaging of The Cell Sorting Process

Naoki Kataoka,[1] Koji Saito,[2] and Yasuji Sawada[1,*]

[1]*Research Institute of Electrical Communication, Tohoku University, Sendai, Japan*
[2]*Advanced Technology Research Laboratories, Nippon Steel Corporation, Kawasaki, Japan*

(Received 13 April 1998)

We present the first NMR microimaging and analysis of cell sorting in a three-dimensional aggregate of dissociated hydra cells by using the stimulated echo method together with temperature scheduling of measurement and regeneration phases. The density correlation analysis, transforming the intensity profile to a cell density profile, showed that cell sorting in a natural three-dimensional process proceeds logarithmically with time. Several features leading to regeneration, special for three-dimensional aggregates, were also observed. [S0031-9007(98)08330-6]

PACS numbers: 87.10.+e, 87.17.–d, 87.61.–c

Regeneration of a whole animal from a completely disordered assembly of dissociated cells is one of the most breathtaking phenomena of morphogenesis. Hydra is a highly regenerative animal in that its regeneration into a whole new animal can occur from tissue as small as one-fiftieth of the whole tissue volume [1] or even from a random aggregate of dissociated cells [2–6]. Many processes are involved in regeneration from a random cell aggregate to a whole animal [7], the first of which is cell sorting among endodermal and ectodermal epithelial cells. To date, the experimental studies of cell sorting have been limited to (1) surface observation or two-dimensional projection [5,8,9] in which it has not been possible to observe the internal cell distribution of different types of cells or (2) to the examination of a thin layer of cell aggregate sandwiched between two glass plates [10].

The model [11] of differential adhesion among five interfaces, aided by random pseudopodal cell motion [9,12–17], two homotypic and a heterotypic cell-cell interface and the two cell-culture solution interfaces, has been proposed for understanding the cell sorting process. An elaborated Monte Carlo simulation [18–20] based on a Potts model showed that differential adhesion in fact leads to cell sorting. Although the logarithmic temporal dependence of the cell sorting process measured by heterotypic boundary length predicted in the two-dimensional case [18,19] was experimentally verified [5,9], it does not mean that the mechanism of cell sorting is explained simply by differential adhesion with random force. In fact, direct observation of individual cells in a two-dimensional aggregate showed that small clusters are quickly formed by random motion of cells and that the clusters then deformed irregularly and coagulated with each other by random deformation of the clusters and the accidental contact of neighboring clusters [10]. Collective motion such as the deformation of clusters, necessary for forming large clusters in addition to the diffusion process, is not taken into account in the Monte Carlo simulation. Also, it was not evident whether or not the cell sorting process proceeds with logarithmic time in natural three-dimensional aggregates, experimentally because observation has been limited to two-dimensional projection [9], and numerically due to the limited number of cells in the simulation [20].

Central to understanding the important mechanism of morphogenesis is the direct internal observation of the cell sorting process as it proceeds in a normal regeneration system, and nuclear magnetic resonance (NMR) microimaging [21–24] may be the only experimental method for this purpose currently available [25]. While the oocyte of a single cell [26] and the early cell lineage pattern [26] of Xenopus laevis have been investigated by this method, the distribution of different kinds of component cells and the progress of cell sorting in morphogenesis have never been studied by this method. It was believed that the distinction of one type of cell from another type would be difficult, since they are chemically alike. In this paper we present the first results of NMR microimaging and an analysis of cell sorting in a three-dimensional aggregate of dissociated hydra cells. By transforming the intensity profile to a cell density profile, the analysis of these raw data shows the progress of the cell sorting clearly and quantitatively.

The resolution of the signals between the endodermal and ectodermal epithelial cells (ED and EC cells), and that of the culture solution in which the aggregate is immersed, determines the averaging time necessary to obtain one NMR image for a given regeneration period. The longer the averaging time, the better the resolution if the object is stationary. However, in this present measurement the averaging time is rather limited, since the specimen under observation is undergoing cell sorting which is nonstationary.

We had, therefore, two difficulties to overcome in pursuing the NMR measurement of this cell sorting process. First, because the endodermal cells and ectodermal cells are chemically alike, it was absolutely impossible to distinguish between the two types of cells and the culture solution by the ordinary spin echo method. Also, even the use of the hydra viridissima in this experiment, in which

only ED cells contain symbiotic chlorella, did not improve the signal difference by this method.

Moreover, while microinjection of an impermeable nontoxic agent such as Gd-DTPA-dextran [27] normally would be useful to increase contrast in such cases as the study of single cells and cell lineage, it could not be employed for this cell sorting experiment, in which a great number of cells are involved initially. Second, a difficulty arose from the trade-off between the averaging time and variations in cell arrangement occurring during the cell sorting process.

To overcome these difficulties, we adopted a stimulated echo method [24,26] by which is measured the strength of the spin echoes that is excited by the second pulse and reappears at an echo time after the third pulse. The observation time, the interval between the second and the third, is chosen in correlation with the diffusion times of water in the samples. By selecting the optimal combination of the observation time (150 msec), the repetition time (10 sec), and the echo time (5 msec), three separate values of image strength (approximately 3:2:1) were obtained for three different objects (two kinds of cells and culture medium) which have three different diffusion constants of water in the three objects, respectively.

The NMR microimaging system used in this study consisted of a JEOL α 400 NMR spectrometer fitted with microimaging units and an 89 mm boremagnet. A gradient strength of about 60 G/cm for three directions (X, Y, Z) and a spectral width of 200 kHz were used. $1024(X) \times 1024(Y) \times 16(Z)$ digital complex data points (voxel) were obtained with the resolution 5 μm $\times$ 5 μm in the horizontal plane and 50 μm in the depth. Data acquisition required 2.5 h. Also, because it was not possible to keep the cell aggregate at a low temperature for long periods of time, the experiment was designed with temperature scheduling consisting of an alternative quenching phase for measurement at 3.0 °C for 2.5 h and an annealing phase for cell sorting at room temperature for 15, 30, 60, and 120 min after the first measurement at 15 min of regeneration, which was required for sample mounting. Since it was shown in separate experiments [28] that the regeneration process of the aggregates under the same temperature scheduling proceeded to the cavity formation stage at around 24 h, the sorting observed here was proven normal under severe conditions of temperature cycles.

Figure 1 shows a time series of NMR images of a regenerating cell aggregate, once dissociated from hydra viridissima and reaggregated by centrifugation [2].

Figure 1(a) shows an NMR image at 15 min of regeneration of hydra cell assembly. The image is globally homogeneous with a mixture of dark spots and bright spots. The bright and dark spots correspond, respectively, to the rich area of ED and EC cells, which are spherical during the process of sorting, with a diameter of approximately 20 μm [2]. The other kinds of cells are known to play no significant role in the early stage of regeneration. Closer inspection reveals that even at 15 min of regeneration the ectodermal cells are found to be more abundant than endodermal at the periphery of the aggregate. This means that cell sorting has proceeded already during the sample mounting time before the first measurement at 15 min. This fast process was also noticed in the preceding observation [9,10]. Figure 1(b) shows an NMR image at 30 min of regeneration. The local accumulation of bright spots is enhanced compared to the one in Fig. 1(a). Figure 1(c) shows an NMR image at 60 min of regeneration. It is observed that the outer shape is rounded compared to earlier images. Figure 1(d) shows an NMR image at 240 min. A concentrated bright region in the center of the aggregate is surrounded by a layer with high density of the ectodermal cells. The thickness of the ectodermal cell layer varies from 30 to 70 μm and in some places greater than 100 μm. It is known that EC cells in the peripheral monolayer of an intact hydra are elongated approximately 50 μm to the radial direction. Therefore, the ectodermal cells in the peripheral layer are still in the process of forming a monolayer at this time.

In order to obtain the signal intensities for unit volume of ED cells and EC cells, we construct a histogram of voxel numbers for various values of the signal intensity from 0 to 255 levels for five regeneration times. The most plausible assumption we can make is that the highest cutoff intensity in each histogram should correspond to that of pure ED cells and that the intensity at the boundary between the background and the cell aggregate should correspond to pure EC cells.

Once the signal intensities for a unit volume of a pure ED and EC cell are obtained, the fractional cell numbers of the ED and EC cells in ith voxel volume will immediately be derived for each voxel. The data were thus transformed from the intensity distribution of the NMR signal (Fig. 1) to the cell number distribution of given kinds of cells.

To illustrate the degree of cell sorting quantitatively we calculated the density correlation length of the endodermal cells, equivalent to the mean distance between them, in the measured plane as a most plausible measure for characterization of cell sorting, defined as

$$L = \Sigma(i, j)X(r_i)\,|r_i - r_j|X(r_j)/\Sigma(i, j)X(r_i)X(r_j)\,, \quad (1)$$

where $X(r_i)$ is the local volume of the endodermal epithelial cells in ith voxel, and r_i is the position vector of ith voxel in the measured plane.

Figure 2 shows the time dependence of the correlation length of the endodermal cell density in the measured plane. Initial distribution is approximately equal to the value calculated for the ideally random case of the cell mass studied. The present data show not only qualitatively that sorting proceeds quickly at the early

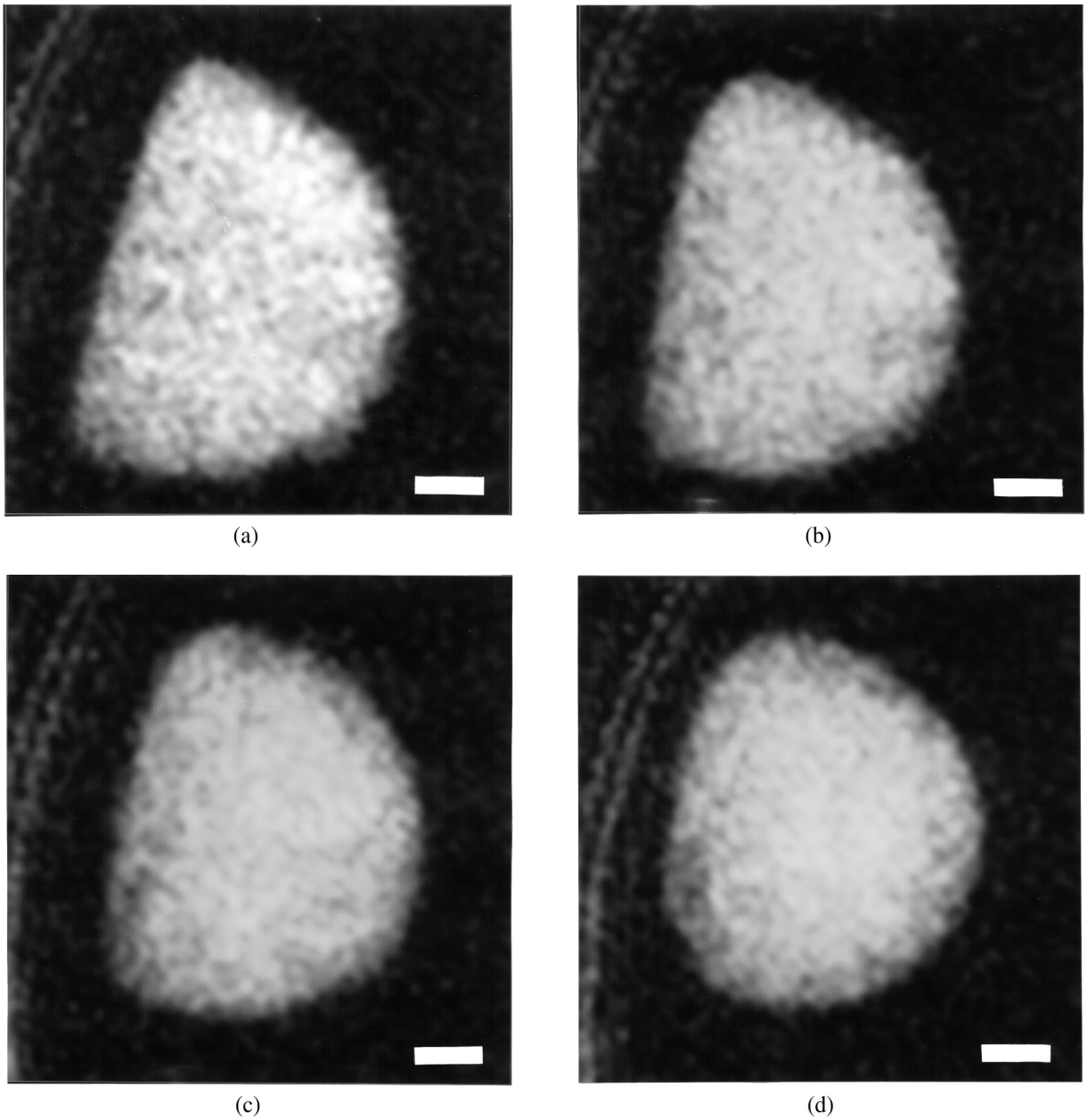

FIG. 1. A time series of NMR images of a regenerating cell aggregate. (a) 15 min, (b) 30 min, (c) 60 min, and (d) 240 min. Scale bar shows 200 μm. The resolution was 5 μm $\times$ 5 μm in the horizontal plane and 50 μm in the depth.

stage and shows down at the later stage, consistent with the earlier indirect data [5,9], but also provide direct evidence that cell sorting proceeds linearly with logarithmic time in three-dimensional cell aggregates.

At 240 min, the change of correlation length achieved approximately 75% of the value of the perfectly sorted case. Cryosections of the aggregate (not shown), which can be obtained only at different times for different samples [29], also showed that cell sorting in hydra proceeds only up to a certain stage where the random mixture of endodermal and ectodermal cells remains in the internal region, before proceeding to the cavity formation process [7]. The gyration radius for the distribution of the endodermal cells was found to show a similar logarithmic dependence on time with the correlation length.

Now let us compare the present results of cell sorting in three-dimensional aggregates with those in two-dimensional aggregates prepared between two glass plates [10]. A single cluster of endodermal cells was observed at the later stage in the present experiment, while several separated clusters were observed at the inner region of the cell assembly in the two-dimensional experiment. This suggests a larger diffusion constant of single cells and a more active deformation of cell clusters

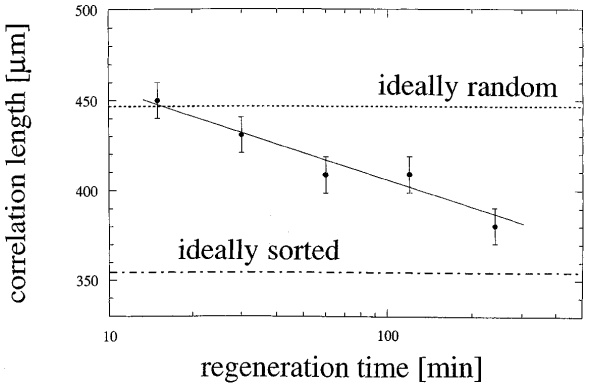

FIG. 2. The time evolution of the correlation length, or equivalently, the mean distance between the cells of the endodermal cells in the measured plane, defined by Eq. (1) in the text, as a most plausible measure for characterizing the degree of cell sorting.

in a three-dimensional cell aggregate. This is reasonable, considering the greater freedom of motion in a three-dimensional cell aggregate compared to that in a two-dimensional cell aggregate. Also, a well-defined, ectodermal interfacial layer observed at 240 min, which is not generally observed in a two-dimensional cell aggregate [10], is consistent with formation of the septate junctions normally expected in the early stage of regeneration from a dissociated cell aggregate [30]. The difference is directly related to the fact that the three-dimensional aggregate can proceed to the cavity formation process and then to the regeneration of a multicellular organism, while the two-dimensional aggregate cannot proceed to the next stage and eventually disintegrates.

Present experimental data did not clarify the microscopic mechanism of sorting [31] because of a long averaging time required for this particular system, but it showed for the first time the global features of cell sorting inside the three-dimensional aggregate.

One of the authors (Y. S.) thanks Dr. T. Murata and Dr. N. Okumura of the Advanced Technology Research Laboratories, Nippon Steel Corporation, for the hospitality during his stay; and E. Mori for a critical reading of the manuscript.

*Author to whom correspondence should be addressed. Electronic address: sawada@sawada.riec.tohoku.ac.jp

[1] H. Shimizu, Y. Sawada, and T. Sugiyama, Dev. Biol. **155**, 287 (1993).
[2] A. Gierer, S. Berking, H. Bode, C. N. David, K. Flick, G. Hansmann, H. Schaller, and E. Trenkner, Nature (London) New Biol. **239**, 98 (1980).
[3] M. Sato and Y. Sawada, Dev. Biol. **133**, 119 (1989).
[4] M. Sato, H. Bode, and Y. Sawada, Dev. Biol. **141**, 412 (1990).
[5] U. Technau and T. Holstein, Dev. Biol. **151**, 117 (1992).
[6] T. Itayama and Y. Sawada, J. Exp. Zool. **273**, 519–526 (1995).
[7] Y. Sawada, M. Sato, and T. Itayama, *Physics of The Living State*, edited by T. Musha and Y. Sawada (IOS Press, Ohmusha, 1994), p. 163.
[8] P. B. Armstrong, Crit. Rev. Biochem. Mol. Biol. **24**, 119 (1989); J. P. Trinkhaus and J. P. Lentz, Dev. Biol. **9**, 115 (1964).
[9] J. C. Mombach, J. A. Glazier, R. C. Raphael, and M. Zajac, Phys. Rev. Lett. **75**, 2244 (1995).
[10] J. P. Rieu, N. Kataoka, and Y. Sawada, Phys. Rev. E **57**, 924 (1998).
[11] M. S. Steinberg, Science **141**, 401 (1963).
[12] M. S. Steinberg and D. R. Garrod, J. Cell Sci. **18**, 403 (1975); D. R. Garrod and M. S. Steinberg, J. Cell Sci. **18**, 405 (1975).
[13] P. Bongrand, *Physical Basis of Cell-Cell Adhesion* (CRC, Boca Raton, FL, 1988).
[14] F. Graner, J. Theor. Biol. **164**, 455 (1993).
[15] F. Graner and Y. Sawada, J. Theor. Biol. **164**, 477 (1993).
[16] M. Maeda-Sato, M. Uchida, F. Graner, and H. Tashiro, Dev. Biol. **162**, 77 (1994).
[17] R. A. Foty, C. M. Pfleger, G. Forgacs, and M. S. Steinberg, Development **122**, 1611 (1996).
[18] F. Graner and J. A. Glazier, Phys. Rev. Lett. **69**, 2013 (1992).
[19] J. A. Glazier and F. Graner, Phys. Rev. E **47**, 2128 (1993).
[20] J. A. Glazier, R. C. Raphael, F. Graner, and Y. Sawada, in *Interplay of Genetic and Physical Processes in the Development of Biological Form*, edited by D. Beysens, G. Forgacs, and F. Gaill (World Scientific, Singapore, 1995), pp. 54–61.
[21] P. C. Lauterbur, Nature (London) **242**, 190 (1973).
[22] P. T. Callaghan, *Principles of Nuclear Magnetic Resonance Microscopy* (Claredon Press, Oxford, 1991).
[23] B. Bluemich and W. Kuhn, *Magnetic Resonance Microscopy* (VCH, Weinheim, 1992).
[24] J. H. Strange, Magn. Reson. Imaging **12**, 161 (1994).
[25] The use of a conventional confocal microscope in hydra cells has given us optical sections only to the depth of approximately 100 μm, which was not deep enough for the study of three-dimensional aggregates. A two-photon confocal microscope recently developed might also work for the present purpose.
[26] J. B. Aguayo, S. J. Blackband, J. Schoeniger, M. A. Martingly, and M. Hintermann, Nature (London) **322**, 190 (1986).
[27] Z. H. Cho, C. B. Ahn, S. C. Juh, I. M. Jo, R. M. Friedenberg, S. E. Fraser, and R. E. Jacob, Philos. Trans. R. Soc. London A **333**, 469 (1990).
[28] N. Kataoka, Ph.D. thesis, Tohoku University, 1997 (unpublished).
[29] T. Mizuguchi, Ph.D. thesis, Tohoku University, 1996 (unpublished).
[30] R. L. Wood and A. M. Kuda, J. Ultrastruct. Res. **70**, 104 (1980).
[31] During the revising process of the paper we were informed of a recent study of cadherin mediated differential adhesion mechanism of cell sorting [D. Godt and U. Tepass, Nature (London) **395**, 387 (1998)].